

©2019, Elsevier. Licensed under the Creative Commons Attribution-NonCommercial-NoDerivatives 4.0 International <http://creativecommons.org/about/downloads>



# **<sup>1</sup>H NMR quantification of spray dried and spray freeze-dried saccharide carriers in dry powder inhaler formulations**

Mai Babenko<sup>1</sup>, Jean-Marie R. Peron<sup>1</sup>, Waseem Kaialy<sup>2</sup>, Gianpiero Calabrese<sup>1</sup>, Raid G Alany<sup>1</sup>, Amr ElShaer<sup>1,\*</sup>

<sup>1</sup> Drug Discovery, Delivery and Patient Care (DDDP) Theme, School of Life Sciences, Pharmacy and Chemistry, Department of Pharmacy, Kingston University London, Kingston upon Thames, Surrey, KT1 2EE

<sup>2</sup> School of Pharmacy, Faculty of Science and Engineering, Wolverhampton University.

\*Corresponding authors:

Dr Amr ElShaer

Drug Discovery, Delivery and Patient Care (DDDP) Theme

School of Life Sciences, Pharmacy and Chemistry

Kingston University London

Penrhyn Road, Kingston upon Thames,

Surrey, KT1 2EE, UK

Email: a.elshaer@kingston.ac.uk

T +44 (0)20 8417 7416 (Internal: 67416)

## **Abstract**

Quantitative analysis using proton NMR (<sup>1</sup>H qNMR) has been employed in various areas such as pharmaceutical analysis (e.g., dissolution study), vaccines, natural products analysis, metabolites, and macrolide antibiotics in agriculture industry. However, it is not routinely used in the quantification of saccharides in dry powder inhaler (DPI) formulations. The aim of this study was to develop a <sup>1</sup>H NMR method for the quantification of saccharides employed in DPI formulations. Dry powders as DPI carriers were prepared by spray drying (SD) and spray freeze drying (SFD) using three saccharides: namely D-mannitol, D-sorbitol and D-(+)-sucrose. The calibration curves constructed for all three saccharides demonstrated linearity with R<sup>2</sup> value of 1. The <sup>1</sup>H qNMR method produced accurate (relative error %: 0.184-3.697) and precise data with high repeatability (RSD %: 0.517-3.126) within the calibration curve concentration range. The <sup>1</sup>H qNMR method also demonstrated significant sensitivity with low values of limit of detection (0.058 mM for D-mannitol, 0.045 mM for D-(+)-sucrose, and 0.056 mM for D-sorbitol) and limit of quantitation (0.175 mM for D-mannitol, 0.135 mM for D-(+)-sucrose, and 0.168 mM for D-sorbitol). Pulmonary deposition via impaction experiments of the three saccharides was quantified using the developed method. It was found that SFD D-mannitol (68.99%) and SFD D-(+)-sucrose (66.62%) exhibited better delivered dose (total saccharide deposition in throat and all impactor stages) than SD D-mannitol (49.03%) and SD D-(+)-sucrose (57.70%) (p< 0.05). The developed <sup>1</sup>H qNMR methodology can be routinely used as an

analytical method to assess pulmonary deposition in impaction experiments of saccharides employed as carriers in DPI formulations.

**Keywords:** Quantitative NMR, Saccharides, Dry powder inhaler formulation, Lung deposition, Spray drying, Spray freeze drying

## 1. Introduction

During the development of DPI formulations, only small amounts of drugs are used; therefore, the overall DPI performance is dependent on the excipients (Pilcer, and Amighi, 2010; Rahimpour, Kouhsoltani and Hamishehkar, 2014). Therapeutic efficacy of DPI formulations is dependent on the amount of the drug dose that reach the lungs (Yang, Chan and Chan, 2014; Ali and Gary, 2015). In the development of carrier based DPI formulations, carrier physicochemical properties such as particle size distribution and surface properties have a significant effect on the drug aerosolisation efficiency and affect the deposition pattern of the therapeutic drug in the lungs (Hamishehkar et al., 2010; Pilcer, and Amighi, 2010; Kaialy and Nokhodchi, 2012; Rahimpour, Kouhsoltani and Hamishehkar, 2014; Ali and Gary, 2015; Banga, 2015; Peng *et al.*, 2016). The deposition patterns of carriers in the respiratory system are an important aspect of the formulation process during the development phase. Anatomical and physiological variabilities within subjects, who have different airways geometry and inhalation profiles (e.g., inspiratory flow rate) also influence the deposition pattern resulting in inconsistent lung drug delivery and poor DPI formulation performance (Depreter, Pilcer and Amighi, 2013; Ung *et al.*, 2014; Ali and Gary, 2015; Banga, 2015). It is difficult to measure the drug dose deposition and the distribution of the aerosolised particle deposition in the lungs *in vivo*. This leads to limited knowledge of the aerosolised DPI formulation performance under real clinical conditions (Ung *et al.*, 2014; Ali and Gary, 2015). The particle size distribution of the aerosolised dry powders dispersed from a DPI is generally studied *in vitro* using an impactor such as a next generation impactor (NGI) (Ung *et al.*, 2014; Ali and Gary, 2015). The NGI has seven stages (1-7) and a micro orifice collector (MOC) arranged in descending cut-off aerodynamic particle size order that separates the largest particles first and pass through the smaller particles to the next NGI stage and determines particle size distributions *in vitro* (D'Addio *et al.*, 2013; Ali and Gary, 2015). The aerosolisation performance of DPI formulations is assessed by mass median aerodynamic diameter (MMAD) along with geometric standard deviation (GSD), fine particle dose (FPD) and fine particle fraction (FPF). MMAD is defined as the aerodynamic diameter at which 50% of total particles by mass (Niwa, Mizutani and Danjo, 2012) and GSD is expressed as a degree of an aerodynamic particle size distribution (Razavi Rohani, Abnous and Tafaghodi, 2014; Ali and Gary, 2015). FPD is defined as the amount of the delivered drug dose with less than or equal to 5.0  $\mu\text{m}$  aerodynamic diameter. FPF is defined as the mass fraction of the delivered drug dose with less than or equal to 5.0  $\mu\text{m}$  aerodynamic diameter and used to characterise the lung deposition and efficiency of DPI formulations for systemic pulmonary application (Kramek-Romanowska *et al.*, 2011; Depreter, Pilcer and Amighi, 2013; Ali and Gary, 2015; Peng *et al.*, 2016; Mönckedieck et al., 2017). Particles collected from the low impactor stages (e.g., between 3 and 5) with less than or equal to 5.0  $\mu\text{m}$  aerodynamic diameter generally represent the respirable-sized drug dose, whereas particles deposited in the higher impactor stages (e.g., throat and stage 1) represent the oropharyngeal deposition in the oropharynx region (Niwa, Mizutani and Danjo, 2012; Ali and Gary, 2015). In order to achieve therapeutic efficacy, the size of drug particles should be respirable (MMAD  $\leq 5.0 \mu\text{m}$ ) with low GSD indicating monodisperse particle size distribution to reach the desired deep lung regions for systemic pulmonary delivery and FPF should be high for drug aerosolisation efficiency

(Kramek-Romanowska *et al.*, 2011; Maltesen, Weert and Grohgan, 2012; Walters *et al.*, 2014; Yang, Chan and Chan, 2014; Rahimpour, Kouhsoltani and Hamishehkar, 2014; Ali and Gary, 2015; Banga, 2015; Peng *et al.*, 2016).

However, the respirable-sized drug particles (MMAD  $\leq 5.0 \mu\text{m}$ ) are associated with high surface energy where inter-particulate forces are involved such as micronised drug to drug cohesive forces. It causes the drug particles to aggregate and leads to limited fluidisation and dispersion of the particles (Pilcer and Amighi, 2010; Ali and Gary, 2015; Berkenfeld, Lamprecht and McConville, 2015; Peng *et al.*, 2016). Therefore, carriers (e.g., particle size 50-100  $\mu\text{m}$  or larger up to 200  $\mu\text{m}$ ) regarded as key components in the development of DPI formulations are employed as a means of delivering the drug to the lungs and to improve the drug delivery efficiency (Kramek-Romanowska *et al.*, 2011; Karner, Littringer and Urbanetz, 2014; Ali and Gary, 2015; Peng *et al.*, 2016; Mönckedieck *et al.*, 2017). Due to the safety concern about carriers to the lungs and insufficient toxicology data, the amount of carriers used should be minimised in DPI formulations to reduce adverse effects of carriers (e.g., cough) (Balducci *et al.*, 2014; Santos and Edelman, 2014; Al-Tabakha, 2015; Peng *et al.*, 2016). Coarse carrier particles used in DPI formulations are designed not to reach the lungs and cleared by swallowing (Peng *et al.*, 2016). Therefore, only the drug particles detached from the carriers during inhalation should be delivered to the deep lung regions (Peng *et al.*, 2016). The evaluation study based on surrogate modelling technique of carrier physicochemical properties (e.g., particle size and surface morphology) reported by Farizhandi *et al.* (2019) showed that the presence of fine carrier particles ( $< 10 \mu\text{m}$ ) could improve FPF (the efficiency of drug aerosolisation). However, inhalation of fine carrier particles might cause irritation, coughing or bronchoconstriction (Peng *et al.*, 2016).

Many analytical methods such as high performance liquid chromatography (HPLC), UV spectroscopy and gas chromatography (GC) have been employed to quantify saccharides (Schmid *et al.*, 2016; Chiara *et al.*, 2017). D'Addio *et al.* (2013) reported the quantification of mannitol deposition via the NGI studies using HPLC with a refractive index detector. However, with these analytical methods routine quantitative analysis of saccharide in the DPI formulation development can be limited due to the lack of chromophores in saccharides (Coombes *et al.*, 2014; Schmid *et al.*, 2016). Gas chromatography and UV spectroscopy involve several steps such as derivatisation to volatilise the compounds for GC and to convert saccharides to UV detectable saccharides (Schmid *et al.*, 2016; Chiara *et al.*, 2017). These methods are regarded as time-consuming. Although derivatisation steps are not required for HPLC, HPLC is associated with low detection sensitivity due to the lack of chromophores on sugars where specialised (and sometimes expensive) detectors are required (Chiara *et al.*, 2017). On the contrary,  $^1\text{H}$  qNMR offers advantages, such as relatively short analysis time and simple sample preparation (simple sample dissolution in a suitable NMR solvent) due to no derivatisation steps involved, and simultaneous analysis of multiple analytes with one internal standard (Holzgrabe, 2010; Bharti and Roy, 2012; Pauli *et al.*, 2012; Hou *et al.*, 2014; Simmler *et al.*, 2014; Chiara *et al.*, 2017).  $^1\text{H}$  qNMR measurements are also reproducible with high accuracy and precision (Bharti and Roy, 2012; Pauli *et al.*, 2012; Sterling *et al.*, 2013; Yamazaki and Takatsu, 2014; Schievano, Tonoli, and Rastrelli, 2017; Wallmeier *et al.*, 2017).

$^1\text{H}$  qNMR represents the direct proportional relationship between the intensity of the signal and the number of protons that gives rise to that signal in the proton NMR spectrum (Holzgrabe, 2010; Richards and Hollerton, 2011; Bharti and Roy, 2012; Günther, 2013; Simmler *et al.*, 2014; Coombes *et al.*, 2014; Hou *et al.*, 2014; Yamazaki and Takatsu, 2014). Therefore,  $^1\text{H}$  qNMR is performed by comparing the integrated signals of the compound of interest with the signals of the internal standard where its structure and purity are known (Pauli *et al.*, 2012; Simmler *et al.*, 2014; Yamazaki and Takatsu, 2014) and have been employed in various areas. Quantification of saccharides (glucose, sucrose and fructose) in Açai raw materials using the absolute intensity qNMR method has been reported by Sterling *et al.* (2013) who demonstrated the accuracy and precision of the method. Quantification of avermectin B<sub>1a</sub> (macrolide antibiotic) in agriculture industry reported by Hou *et al.*

(2014) showed no significant difference between HPLC and  $^1\text{H}$  qNMR quantitation results. Dissolution study using  $^1\text{H}$  NMR reported by Coombes *et al.* (2014) demonstrated high selectivity to quantify the mixture of three active drug substances and excipient (lactose) in oral immediate-release tablets with sufficient sensitivity in the low concentrations ( $6\ \mu\text{g mL}^{-1}$  as maximum concentration). Identification and quantitation of sugars excipients (mannitol, sucrose, trehalose and lactose) in freeze-dried vaccines using Total Correlation Spectroscopy (TOCSY) 2D NMR techniques was reported by Duru *et al.* (2015). Schievano *et al.* (2017) reported 22 sugars (e.g., glucose, sucrose, and trehalose) that were present in honey samples prepared in buffer and were able to identify and quantify them using Chemical Shift Selective Filters TOCSY (CSSFs-TOCSY). The CSSFs-TOCSY technique proved to be an accurate and precise quantitative analytical tools with easy sample preparation. Although there are many precedents indicating the usefulness of NMR techniques,  $^1\text{H}$  qNMR is not routinely used in the quantification of saccharides in DPI formulations. So far, no studies reported the use of  $^1\text{H}$  qNMR to quantify the deposition of saccharides in pulmonary formulations. The aim of this study was to develop an analytical method using  $^1\text{H}$  NMR spectroscopy for quantitative analysis of saccharide deposition patterns. Spray drying and spray freeze drying using D-mannitol, D-sorbitol and D-(+)-sucrose were employed to prepare saccharide dry powders as DPI carriers. Impaction studies were carried out employing a next generation impactor (NGI) with an Alberta Idealised Throat (AIT) to estimate the lung deposition patterns *in vitro* for saccharide DPI formulations.

## **2. Materials and methods**

### **2.1. Materials**

D-mannitol (mannitol, purity 98%, Sigma-Aldrich), D-sorbitol (sorbitol, purity 98%, Sigma-Life Science), D-(+)-sucrose (sucrose, purity 99.7%, Acros Organics), sodium benzoate (purity 99%, Sigma-Aldrich), deuterium oxide ( $\text{D}_2\text{O}$ , Euriso-top®), sodium 3-trimethylsilyl propionate-2,2,3,3- $\text{d}_4$  (TSP, Merck Sharp & Dohme Canada Limited), and human recombinant insulin (Sigma-Aldrich).

### **2.2. Spray drying**

Saccharides aqueous solutions (15% w/v) were prepared at room temperature and spray dried using a Büchi Mini Spray Dryer B-290 (Flawil, Switzerland) under the optimised processing parameters:  $320\ \text{mL hr}^{-1}$  feeding rate, spray flow rate with compressed air between 473 and  $601\ \text{L hr}^{-1}$ , 100% aspirator speed setting, inlet temperature at  $130^\circ\text{C}$  and outlet temperature at  $70\pm 5^\circ\text{C}$ . Output pressure and receiver pressure were set to 4 and 8 bar, respectively.

### **2.3. Spray freeze drying**

Saccharides aqueous solutions (15% w/v) were sprayed over a cryogenic medium composed of liquid nitrogen ( $\text{LN}_2$ ) in a 250 mL round bottom flask. The samples were freeze dried using BenchTop Pro with Omnitronics™ (SP Scientific, UK) for 48 hours at  $55\pm 5\ \mu\text{bar}$  pressure and condenser temperature of  $-59\pm 2^\circ\text{C}$ .

### **2.4. Morphology by scanning electron microscopy**

Morphology along with particle size of all three selected raw saccharides (mannitol, sucrose, and sorbitol), spray dried (SD) and spray freeze dried (SFD) mannitol and sucrose dry powders were characterised by scanning electron microscopy (SEM, ZEISS EVO®50, UK). Double-sided cohesive carbon tabs were adhered to aluminum stubs and all dry powder samples were placed onto the carbon tabs. Any excess powder samples were tapped off from the tabs. These samples were then coated with a palladium/gold alloy using a SC7640 Sputter Coater under Argon gas for 2 minutes. Multiple images of coated samples were then captured for each sample using SEM.

### **2.5. Particle size distribution by laser diffraction**

Particle size distribution of all three selected raw saccharides (mannitol, sucrose, and sorbitol), SD and SFD mannitol and sucrose dry powders was measured using a HELOS/BF laser diffraction system equipped with a Rodos dispenser (Sympatec GmbH, Clausthal-Zellerfeld, Germany) and vibratory feeding unit (VIBRI, Sympatec GmbH, Clausthal-Zellerfeld, Germany) in the R3 measuring range from 0.5/0.9 to 175  $\mu\text{m}$ . The trigger condition for normal measurement under the standard mode was set to start after the “channel 21” was  $\geq 1.0\%$  and stop after the optimal concentration was  $\leq 1.9\%$  for 10 sec real time or 60 sec trigger time out. The primary pressure was set to 1.0 bar. Sympatec WINDOX software was used to calculate volume median diameter (VMD).

### **2.6. Thermogravimetric analysis**

Thermogravimetric analysis (TGA) for all three selected raw saccharides (mannitol, sucrose, and sorbitol), SD and SFD mannitol and sucrose dry powders was performed to measure moisture content using a METTLER TOLEDO TGA/DSC1 STARe System (Mettler Toledo, Switzerland). All dry powder samples weighted between 4.5 mg and 12.0 mg were loaded onto a pan and heated under nitrogen gas in the temperature range from 40 °C to 400 °C. The TGA curves were recorded at room temperature in an inert atmosphere using STARe Software version 8.10.

### **2.7. Pulmonary deposition study by next generation impactor**

Pulmonary deposition was studied using a NGI (Copley Scientific, Nottingham, UK) equipped with the Alberta Idealised Throat (AIT) 28028 designed for adult human upper respiratory tract geometry. The airflow of the NGI was adjusted to  $30 \pm 0.5 \text{ L min}^{-1}$  with 3 sec inspiration time. A leak test was performed on the NGI prior to each use. In this study, Handihaler® (Boehringer Ingelheim, Germany) was used to deliver the content of raw, SD and SFD saccharide dry powders filled using size 3 capsules (CAPSUGEL®, UK) during the impaction studies. The saccharide dry powders deposited on AIT and on all NGI stages (stages 1-7 and micro orifice collector, MOC) were collected, washing with distilled water (2 mL) and kept in glass vials in the refrigerator (2-8 °C) prior to  $^1\text{H}$  qNMR analysis. Saccharide dry powders deposited on AIT, 7 stages and MOC in the NGI were based on the aerodynamic cut-off diameters of 0.541  $\mu\text{m}$  (stage 7), 0.834  $\mu\text{m}$  (stage 6), 1.357  $\mu\text{m}$  (stage 5), 2.299  $\mu\text{m}$  (stage 4), 3.988  $\mu\text{m}$  (stage 3), 6.395  $\mu\text{m}$  (stage 2), and 11.719  $\mu\text{m}$  (stage 1) at flow rate of  $30 \text{ L min}^{-1}$  with 3 sec inspiration time. All NGI studies were performed at room temperature and run in triplicate. Saccharide aerosolisation performance was assessed, using Microsoft Excel and Copley Inhaler Testing Data Analysis Software (CITDAS) Version 3.10 Wibu that meets the requirements of USP 32 and Ph.Eur.6.0, to determine the delivered dose expressed as a percentage of the total saccharide deposition on AIT and all the impactor stages, FPF, MMAD and GSD. The delivered dose was determined as the ratio of the total saccharide deposition on AIT and all the NGI stages excluding the deposition in the inhaler device and capsules to the total saccharide dose dispersed from the device including the deposition in the inhaler device and capsules (i.e. the mass of the saccharide filled into the capsule). In this study, FPF, MMAD and GSD determined were based on the saccharide deposition dose.

### **2.8. NMR sample preparation**

Standard stock solutions of each of the three saccharides and internal standard (sodium benzoate) were prepared in distilled water at a concentration of 107.591 mM for mannitol and sorbitol, 58.255 mM for sucrose, and 297.140 mM for sodium benzoate. Five to six serial dilutions were prepared and mixed with sodium benzoate;  $\text{D}_2\text{O}$  was used as solvent spiked with TSP as the chemical shift reference material. Each solution (650  $\mu\text{L}$ ) was transferred into a 5 mm diameter NMR tube and analysed as described in the next section.

NGI sample solutions for  $^1\text{H}$  qNMR were prepared by mixing  $\text{D}_2\text{O}$  with TSP, sodium benzoate and each deposited powders collected from the NGI (AIT, all 7 stages of the NGI impactor and MOC) in ratios of

1:1:8, respectively. The concentration of internal standard was kept constant through all the NMR sample solutions.

## 2.9. <sup>1</sup>H NMR data measurement

All <sup>1</sup>H NMR measurements for standard calibration curves, validation experiments and NGI sample solutions were performed on a Bruker Avance III 600 NMR spectrometer (600.13MHz for <sup>1</sup>H) equipped with a TXI <sup>1</sup>H/<sup>2</sup>D{<sup>13</sup>C, <sup>15</sup>N} autotune room temperature probehead (Bruker UK Limited, Coventry, UK). Water suppression was achieved using that Bruker-supplied noesygppr1d (avance-version 12/01/11) pulse program which performs presaturation of the water signal during the relaxation delay and mixing time and further removes unwanted magnetisation artefacts using a spoil gradient. Acquisition parameters for all <sup>1</sup>H NMR spectra were set as follows: mixing time 10ms, number of scans 64, complex data points 64K for 12KHz spectral width giving an acquisition time of 2.66s. The receiver gain (RG) was limited to a maximum value of 128. In order to mitigate against possible differences in receiver gain within replicates run in automation, an internal standard was used to normalise integrals and thus alleviate integral discrepancies resulting from the non-linearity of the probehead amplifier. The internal standard selected had to be accurately weighed and its concentration was kept constant throughout the measurements. We used readily available sodium benzoate as its resonances were not influenced by the analyte's peaks or the water signal. The internal standard was used purely as an integral normalisation device. The relaxation delay (D1) was set to 4 seconds which overall afforded a repetition time = 6.7s, approx. 3 x T<sub>1</sub> of the slowest relaxing analyte's proton and approximately 1 x T<sub>1</sub> of the slowest relaxing benzoate proton (T<sub>1</sub> values data available in the supplementary information). Temperature was kept constant at 298.2K throughout the NMR measurements. All <sup>1</sup>H NMR measurements were run in triplicate under the same parameters and conditions.

## 2.10. NMR data processing

All NMR data were processed using TopSpin 3.5pl7 (Bruker BioSpin GmbH, Rheinstetten, Germany) by applying a fast Fourier transform with an exponential apodisation window (line broadening of 0.2Hz) and zero filling to 64K real data points. The spectra were automatically referenced to internal TSP, automatically phase corrected with manual fine tuning of the phase as required, and automatically baseline corrected (using polynomial degree 5).

## 2.11. <sup>1</sup>H NMR quantitative analysis

All the signals for the internal standard, sodium benzoate, and each saccharide were manually integrated. One of the peaks from the internal standard was chosen as the calibrant in all the spectra. After completion of manual integration, the integral values for the saccharides were normalised using the calibrant and a calibration curve was constructed for subsequent quantitative analysis of saccharide lung deposition *in vitro*. Calibration curves for three selected saccharides were constructed by plotting the known concentration of saccharide on the x-axis against the normalised integral values of the saccharide on the y-axis. Normalised integral values were calculated using equation 1:

Integral Values (y-axis) =

$$\frac{(\text{Integral Values of Saccharide} / \text{Number of Atoms in Saccharide})}{(\text{Integral Values of Internal Standard} / \text{Number of Atoms in Internal Standard})}$$

*Equation 1*

The magnetisation recovery afforded by a repetition rate of 6.7 second was found to afford a good sensitivity for the saccharides (~ 3 x T<sub>1</sub> of slowest relaxing saccharide proton) and adequate sensitivity for the internal standard (~ 1 x T<sub>1</sub> of slowest relaxing benzoate proton). The T<sub>1</sub> measurement results are provided separately and summarised in Tables S2-S4 in the supplementary information. The internal standard was solely used to derive relative integral values for the saccharides. Although the

maximum sensitivity is not obtained for the analytes in those conditions, quantitative results were obtained, and the time saved thanks to a shorter acquisition allowed for faster sample throughput.

## **2.12. Method validation**

$^1\text{H}$  qNMR method validation was carried out based on the International Council for Harmonisation of Technical Requirements for Pharmaceuticals for Human Use (ICH) guidelines. The main objective was to demonstrate that the  $^1\text{H}$  qNMR analysis was suitable for the quantitation of the saccharide used in our DPI formulations. Validation characteristics, such as specificity, linearity and range, accuracy and precision along with limit of detection (LOD) and limit of quantitation (LOQ) were assessed.

### ***Specificity***

Specificity was evaluated using  $^1\text{H}$  NMR spectra of the three saccharides to see whether the signals of each saccharide, sodium benzoate and water were well separated from each other in all  $^1\text{H}$  NMR spectra. Whilst determining  $T_1$  values we saw no significant changes in peak position, resolution, and  $T_1$  values when measuring the analyte alone (in deuterium oxide) or in the presence of sodium benzoate or insulin (used as model compound) in a similar concentration to those used in the calibration curves (supplementary information, Figures S1 – S7).

### ***Linearity and Range***

The linearity of the  $^1\text{H}$  qNMR method was evaluated by preparing the calibration curves for a series of 5-6 concentrations of selected saccharides. The concentrations ranges were 1.352-21.636 mM for mannitol, 1.351-21.615 mM for sorbitol, and 0.729-23.314 mM for sucrose. Linear regression analysis was used to evidence the direct proportional relationship between the signal intensity and the number of protons. The correlation coefficient ( $R^2$ ) and the regression equation (y intercept and slope of the regression line) were computed.

### ***Accuracy / Trueness***

The accuracy, which is also termed trueness, of the  $^1\text{H}$  qNMR method was assessed by measuring three concentrations (low, middle and high end of the calibration curve concentration range) in three replicates. The accuracy of the measurements was reported as the difference (bias%, relative error%) between the measured concentration ( $mc$ ) and nominal concentration ( $nc$ ) of each saccharide of interest, using the equation:  $(mc-nc) \times 100/nc$  provided by Schievano *et al.* (2017).

### ***Precision***

The intra-day precision was assessed by calculating the standard deviation (SD) and relative standard deviation (RSD%) of the above replicated measurements (three different concentrations/three replicates each on the same day). The inter-day precision of the  $^1\text{H}$  qNMR method in the same laboratory, under the same measurement conditions, was assessed by replicating the same measurements each day for three days. The SD and RSD% of the nine NMR data acquisitions per concentration were calculated.

### ***Limit of detection and limit of quantitation***

The LOD (defined as “the lowest amount of analyte in a sample that can be detected but not necessarily quantitated”) and LOQ (defined as the lower limit of precise and accurate quantitative measurements) were calculated at the 95% confidence level using “Regression statistics analysis” in Excel. The ICH guidelines equations were used:  $\text{LOD} = 3.3 \cdot \sigma / S$  and  $\text{LOQ} = 10 \cdot \sigma / S$ , where  $\sigma$  is the standard deviation of the response and  $S$  is the slope of the calibration curve.



### 3. Results and discussion

#### 3.1. Physicochemical Characterisation

Prior to quantifying the three saccharides using  $^1\text{H}$  qNMR, the morphology, particle size, and moisture content of the raw, SD and SFD dry powders were characterised using SEM, laser diffraction and TGA. Raw sucrose was milled in order to reduce the particle size within the carrier particle size range. Mannitol and sucrose dry powders were successfully prepared as DPI carriers using SD and SFD and characterised. Sorbitol aqueous solution (15% v/w) failed to produce dry powders using SD, which resulted in clear paste formation due to the inlet temperature used at 130 °C (above sorbitol melting point of around 100 °C (Nezzal et al., 2009)). SFD also failed to produce sorbitol dry powders as DPI carrier resulting in collapse due to the primary drying process taking place at room temperature that was above glass transition temperature of sorbitol. Due to the failure of SD and SFD powder formations for sorbitol, physicochemical characterisation was carried out only for raw sorbitol in this study.

##### 3.1.1. Morphology by Scanning Electron Microscopy

Different morphologies in all mannitol dry powder samples were observed (Figure 1). The SEM image of raw mannitol (Figure 1A) showed elongated particles with rather rough surface. It was observed that SD and SFD methods modified the size and surface morphology of mannitol particles. In contrast to SD mannitol powders, the resultant SFD mannitol powders were very fluffy. The SEM image of SFD mannitol (Figure 1B) showed spherical and highly porous particles with large particle size ranging between 50-110  $\mu\text{m}$ , which is within the suitable carrier size range (50-100  $\mu\text{m}$  or larger up to 200  $\mu\text{m}$  as described in introduction). However, some small fragments of the porous particles were also observed and resulted in the broad particle size distribution with the high span value discussed later in section 3.1.2. On the contrary, the SEM image of SD mannitol (Figure 1C) showed spherical particles with smooth surface in the smaller particle size range of 2-10  $\mu\text{m}$ . Spherical particles with smooth surface produced by SD could be due to the conversion of feed solution to droplets exposed to hot compressed air. This leads to instant solvent evaporation and droplets formation with coated surface layer (Razavi Rohani, Abnous and Tafaghodi, 2014).

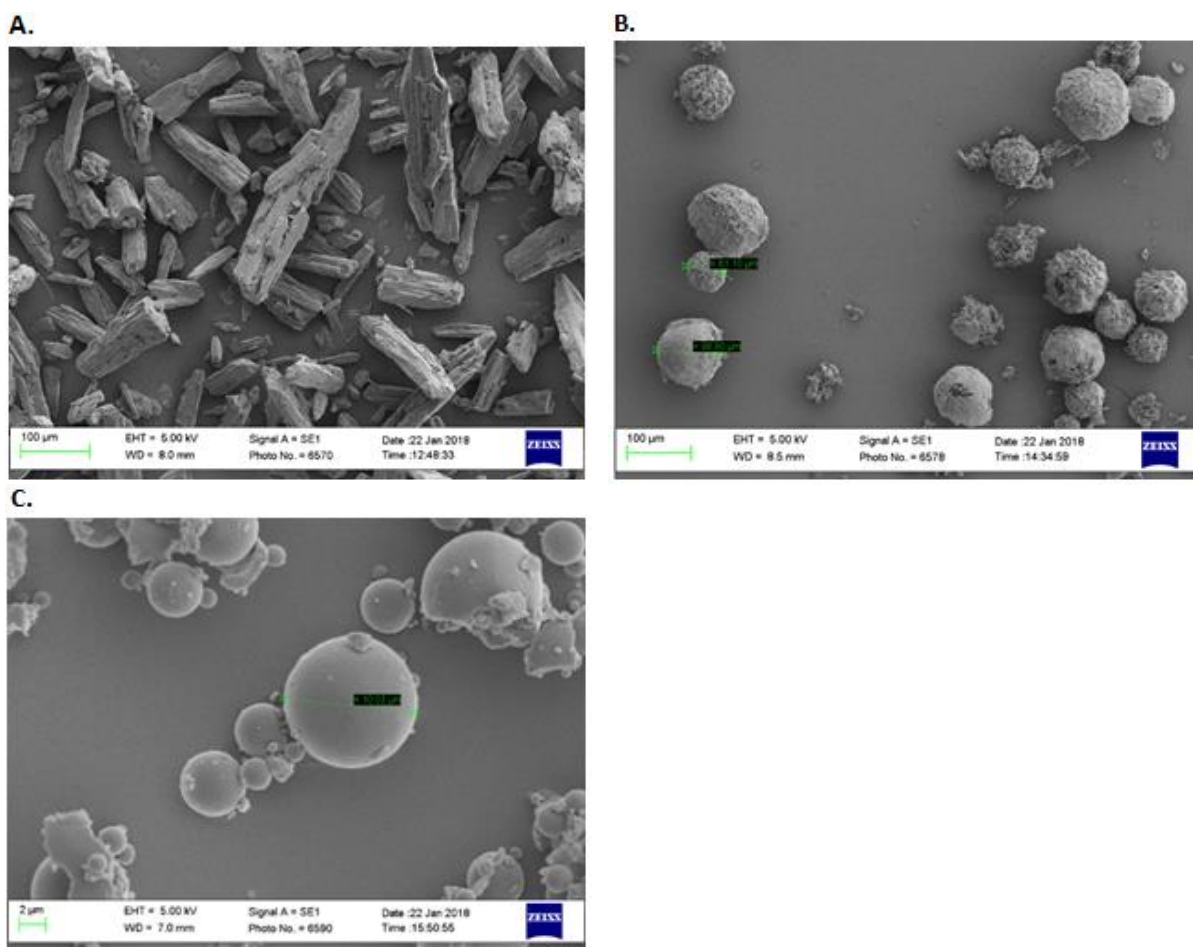


**Figure 1:** SEM images of dry powders of (A) raw mannitol, (B) spray freeze dried (SFD) mannitol and (C) spray dried (SD) mannitol.

Analogously to mannitol, different morphologies in all sucrose dry powder samples were observed (Figure 2). Raw sucrose was elongated particles with rather rough surface in the particle size range of 4-130  $\mu$ m (Figure 2A). On the other hand, SFD sucrose (Figure 2B) showed aggregated particles with smooth surface composed of some spherical and irregular shape particles fusing together. This was due to the aggregation occurred during the process of spraying aqueous saccharide samples over LN<sub>2</sub> and during the primary drying. SD particles also showed aggregation with smooth surface composed of spherical particles fusing together resulting in particles with irregular shape (Figure 2C). Despite the smooth surface observed for both SFD and SD sucrose, the resultant SFD sucrose powders were rather fluffy compared to SD sucrose powders. Nonetheless, it was observed that SFD produced some spherical particles with a suitable carrier particle size range of 50-100  $\mu$ m (Figure 2B) whereas SD method produced spherical particles with the smaller particle size range of 20-100  $\mu$ m (Figure 2C). Raw sorbitol formed irregular particles with fibrous and rather rough surface in the particle size range of 15-150  $\mu$ m (Figure 2D). SEM images showed various morphologies overall and the particle size for all saccharide dry powders varied with the method of dry powder preparation in the following rank order: raw > SFD > SD.

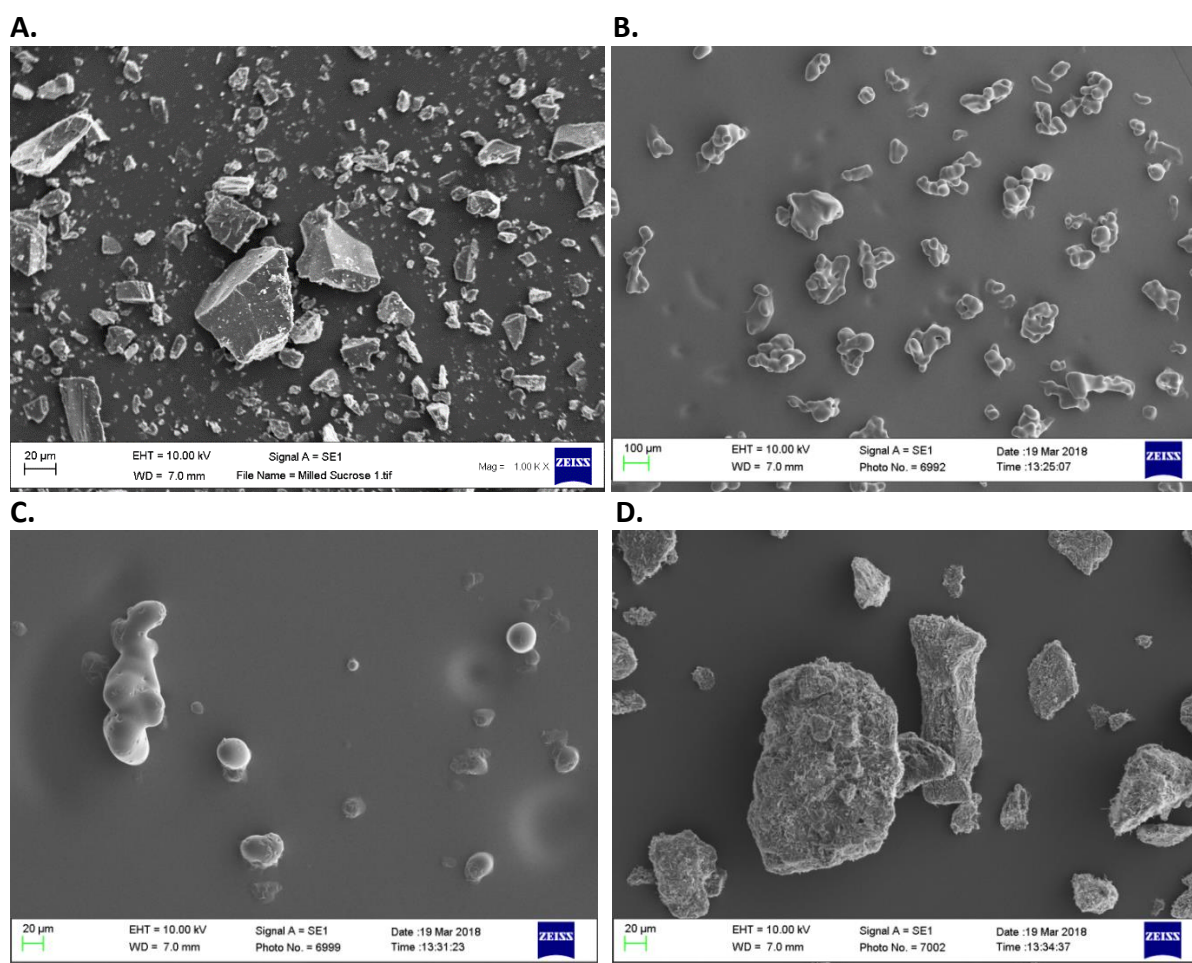


**Figure 2:** SEM images of dry powders of (A) raw sucrose, (B) spray freeze dried (SFD) sucrose, (C) spray dried (SD) sucrose and (D) raw sorbitol.

### 3.1.2. Particle size distribution by laser diffraction

The particle diameters ( $\mu\text{m}$ ) at 10%, 50% and 90% of the volume distribution for raw saccharides (mannitol, sucrose, and sorbitol), SFD and SD mannitol and sucrose dry powders are presented in Table 1. The results of laser diffraction in Table 1 showed that raw saccharides had the largest Volume Mean Diameter (VMD) followed by SFD saccharides and SD saccharides had the smallest VMD in the following rank order: raw sorbitol > raw sucrose > raw mannitol > SFD sucrose > SFD mannitol > SD mannitol > SD sucrose. Particle size measurement by laser diffraction also showed that both methods SFD and SD modified the particle size of saccharide dry powders and supported the SEM images (Figure 1 and 2). The span values were in the rank order of SFD mannitol > SFD sucrose > raw sucrose > raw mannitol > SD sucrose > SD mannitol > raw sorbitol. This represented that raw sorbitol had the most narrow size distribution with the lowest span value (1.29), whereas SFD mannitol had the highest span value of above 10 indicating polydispersity due to the presence of some small fragments of the porous particles observed by the SEM image (Figure 1B). This might have led to the saccharide particle deposition in the lower NGI stages (discussed later in pulmonary deposition). SD saccharides showed narrower particle distribution with the smaller span values compared to their raw and SFD saccharides. As discussed in introduction, particle size distribution affects the deposition pattern in the respiratory system and coarse carrier particles used in DPI formulations should not reach the lungs; therefore, monodisperse size distribution is desirable for carriers targeting the oropharynx region. Broad particle distribution would lead to variations in the deposition pattern in the targeted regions.

**Table 1:** Particle size volume diameters ( $\mu\text{m}$ ) at 10% ( $Dv_{10}$ ), 50% ( $Dv_{50}$ ) and 90% ( $Dv_{90}$ ) of the volume distribution for raw saccharides (mannitol, sucrose, and sorbitol), spray freeze dried (SFD) mannitol and sucrose, and spray dried (SD) mannitol and sucrose dry powders.

Saccharide	$Dv_{10}$ ( $\mu\text{m}$ )	$Dv_{50}$ ( $\mu\text{m}$ )	$Dv_{90}$ ( $\mu\text{m}$ )	VMD ( $\mu\text{m}$ )	Span ( $Dv_{90} - Dv_{10} / Dv_{50}$ )
Raw mannitol	8.87	42.32	103.97	50.20	2.25
SFD mannitol	1.62	10.34	113.37	34.83	10.81
SD mannitol	1.05	4.77	10.87	5.54	2.06
Raw sucrose	4.14	48.98	121.79	56.44	2.40
SFD sucrose	2.62	25.47	99.01	40.11	3.78
SD sucrose	0.87	3.45	8.57	4.17	2.23
Raw sorbitol	17.54	107.59	156.50	94.96	1.29

### 3.1.3. Thermogravimetric analysis

Moisture content in raw, SFD and SD saccharide dry powders was measured by TGA. The TGA results in Figure 3a showed that the weight loss was observed in SFD mannitol (5.5%) and SD mannitol (2.0%) below 70 °C where water evaporation would have taken place whereas there was no mass change observed for raw mannitol. It was also observed that SFD and SD sucrose exhibited weight loss (7.5% and 3.0%, respectively) whereas raw sucrose showed no mass changes (Figure 3b). This indicates that SFD and SD methods produced hygroscopic saccharide formulations compared to raw saccharides (mannitol and sucrose). In contrast to the SD formulations, the higher moisture content was observed in the SFD formulations and this could be linked to the drying process which is not as efficient as the SD which showed lower moisture content. Raw sorbitol is considered as hygroscopic compound due to the weight loss of about 4.0% observed in the TGA result (Figure 3a) compared to raw mannitol and raw sucrose.

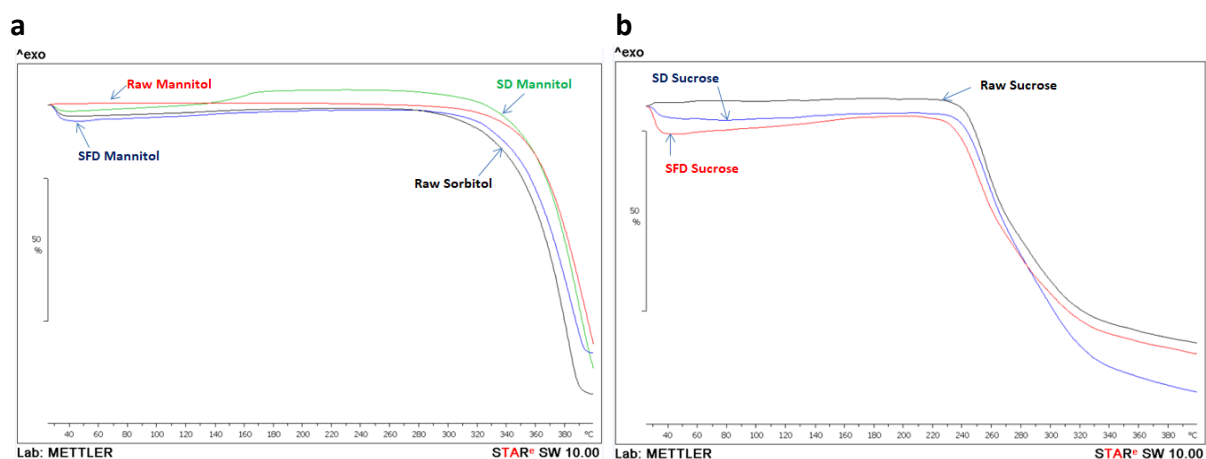


**Figure 3:** Thermogravimetric analysis (TGA) thermograms of (a) raw mannitol, spray freeze dried (SFD) mannitol, spray dried (SD) mannitol, and raw sorbitol, (b) raw sucrose, spray freeze dried (SFD) sucrose and spray dried (SD) sucrose dry powders.

### 3.2. Quantitative proton NMR

#### 3.2.1. Experimental parameters and water suppression

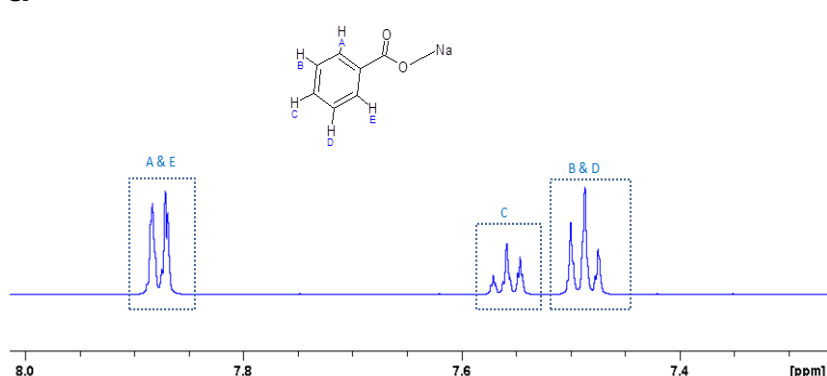
In this study, processing parameters (e.g., signal to noise ratio (S/N)) and acquisition parameters such as number of scans, acquisition time and receiver gain (RG) were pre-optimised as these parameters affect the accuracy and precision of the measurement (Bharti and Roy, 2012). Setting RG to 128 and the number of scans to 64 allowed us to achieve S/N of 250:1 or better (Holzgrabe, 2010; Bharti and Roy, 2012). Acquisition time was 2.656 sec and the relaxation delay was set to 4.000 sec to allow satisfactory relaxation of the protons between pulses (Holzgrabe, 2010; Roberts and Lian, 2011). Temperature, which is known to affect chemical shifts and integration (Bharti and Roy, 2012; Yamazaki and Takatsu, 2014) was kept constant at 298.2K throughout the measurements.  $^1\text{H}$  qNMR measurements were carried out using water suppression for accurate and precise quantification of the signals of interest (Hore, 1983; Holzgrabe, 2010; Richards and Hollerton, 2011; Bharti and Roy, 2012; Coombes *et al.*, 2014; Giraudeau, Silvestre and Akoka, 2015).

#### 3.2.2. Method validation

Quantitative analysis was carried out by comparing the integrated signals of the saccharide of interest with sodium benzoate as an internal standard. Sodium benzoate was chosen as an internal standard as it shows no interference with saccharides and its peaks are well resolved (known requirements for q-NMR) (Holzgrabe, 2010; Bharti and Roy, 2012; Pauli *et al.*, 2012). Sodium benzoate also dissolves well in  $\text{D}_2\text{O}$ , and although it is hygroscopic at humidity above 50%, under normal weighing conditions in an enclosed accurate balance, in our hands it did not pickup significant amount of water.

The reference compound and internal standard were directly added to the saccharide in the same NMR tube and dissolved well in deuterated NMR solvent. Figure 4 shows the  $^1\text{H}$  NMR spectra of sodium benzoate and the three saccharides dissolved in  $\text{H}_2\text{O}/\text{D}_2\text{O}$  with the integral regions selected for quantification. The signals of sodium benzoate were manually integrated in the range of 7.457-7.905 ppm (Figure 4a) and the signal at 7.87 ppm (Figure 4a,  $\text{H}_\text{A}$  and  $\text{H}_\text{E}$  protons, multiplet,  $T_1 = 6.3\text{s}$ ) was selected as internal calibrant peak. The signals of each saccharide were manually integrated in the range of 3.655-3.906 ppm for mannitol (Figure 4b), 3.551-3.900 ppm for sorbitol (Figure 4c) and 3.440-4.247 ppm and 5.396-5.432 ppm for sucrose (Figure 4d).

**a**



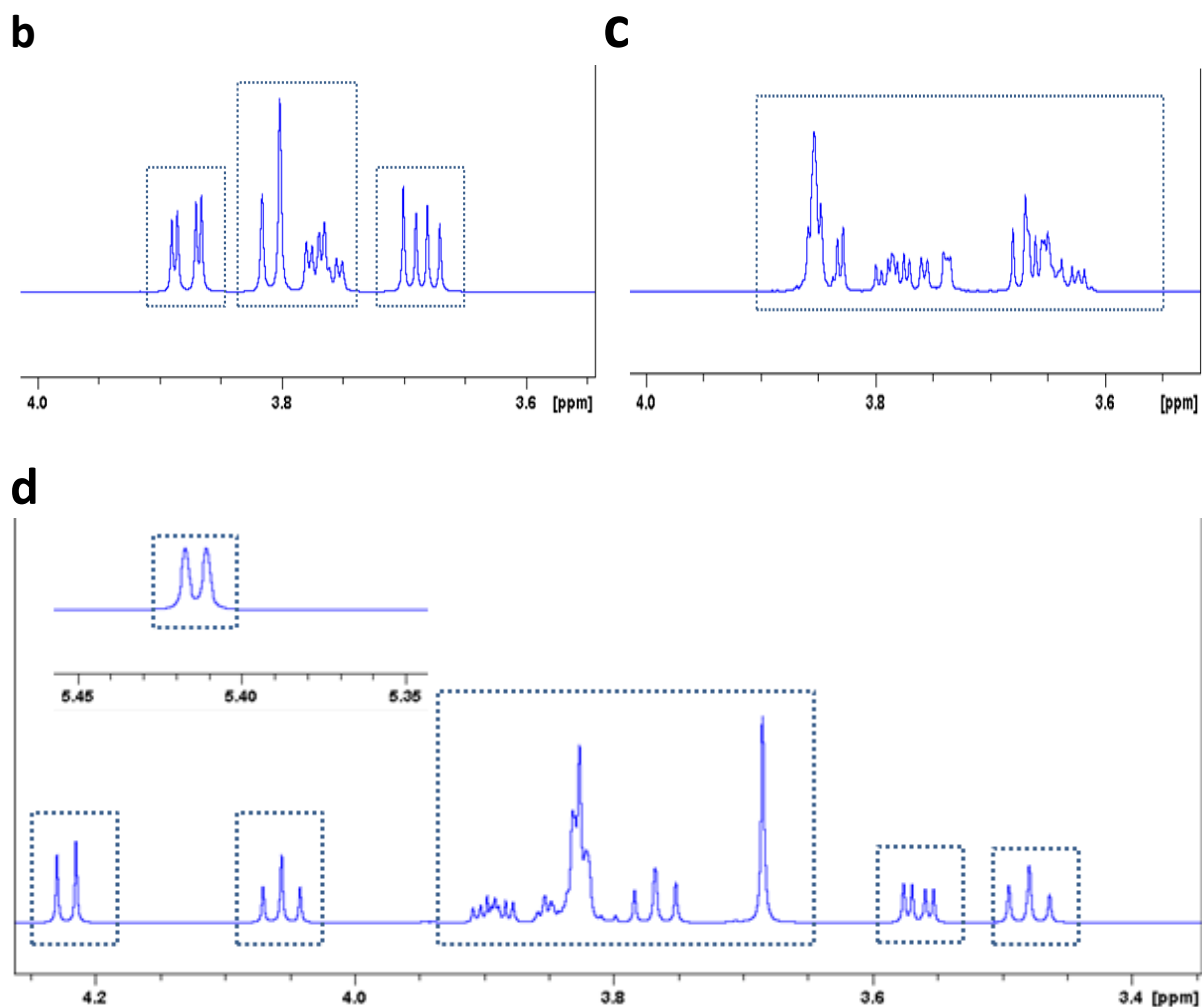


**Figure 4:**  $^1\text{H}$  NMR spectra of (a) sodium benzoate with peak assignments, (b) mannitol, (c) sorbitol, and (d) sucrose in  $\text{H}_2\text{O}/\text{D}_2\text{O}$  (90:10) with the integral regions selected for quantification.

### **Specificity**

The signals of each saccharide, sodium benzoate and water around 4.80 ppm did not overlap in any of the  $^1\text{H}$  NMR spectra (Figure 5) which allowed unequivocal integration of the signals of interest.

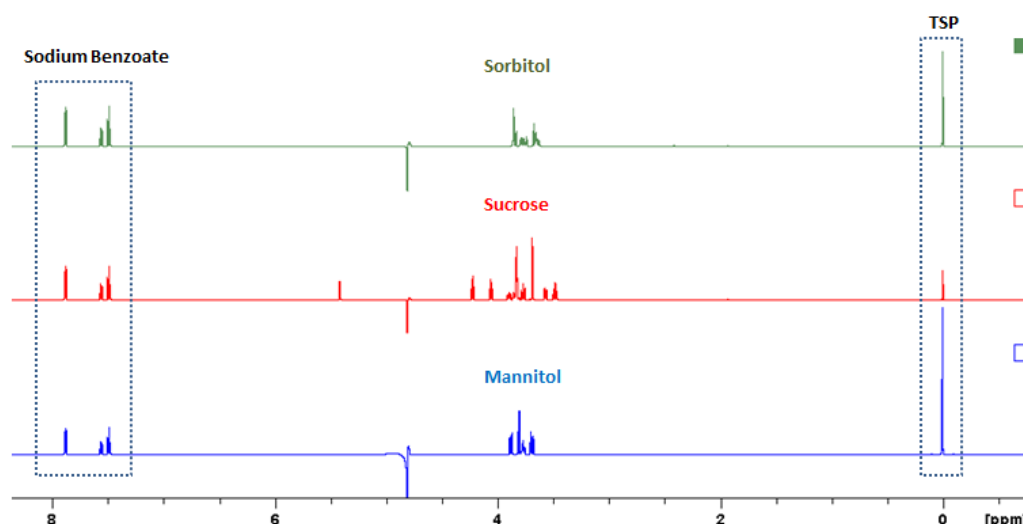


**Figure 5:**  $^1\text{H}$  NMR spectra multiple displays of saccharide samples (mannitol, sucrose, and sorbitol) dissolved in distilled water in the presence of internal standard of sodium benzoate. TSP: Sodium 3-trimethylsilyl propionate-2,2,3,3- $\text{d}_4$ .

### **Linearity and Range**

The linearity was determined by regression analysis that generated linear correlation coefficient ( $R^2$ ) and regression equation with five or six different concentrations (Table 3). The calibration curves constructed for all three saccharides were linear with  $R^2$  value of 1.0000 (Figure 6a). This showed, as expected, that the integral value was proportional to concentration within the range of concentrations chosen. Regression analysis for the determination of correction factors demonstrated no discrepancy as the measured concentration (y-axis) was almost as equal to the nominal concentration (x-axis) (Figure 6b and Table 3).

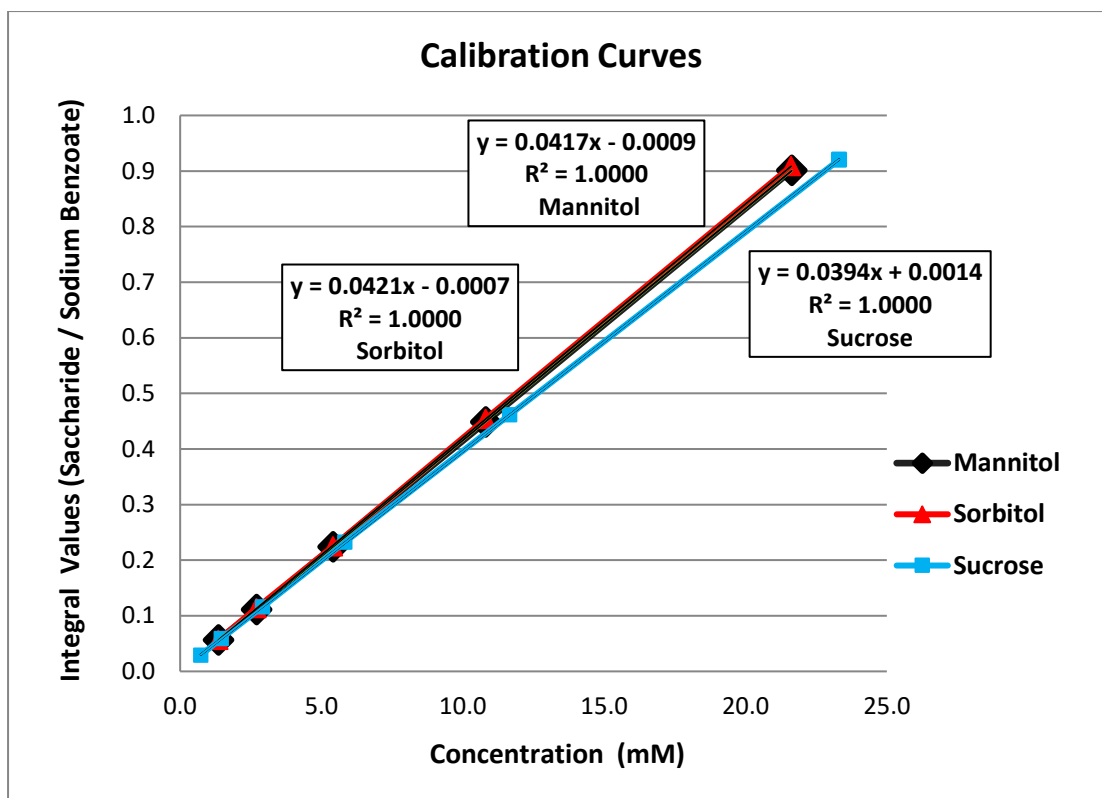


**Figure 6a:** Calibration curves for mannitol, sucrose and sorbitol.

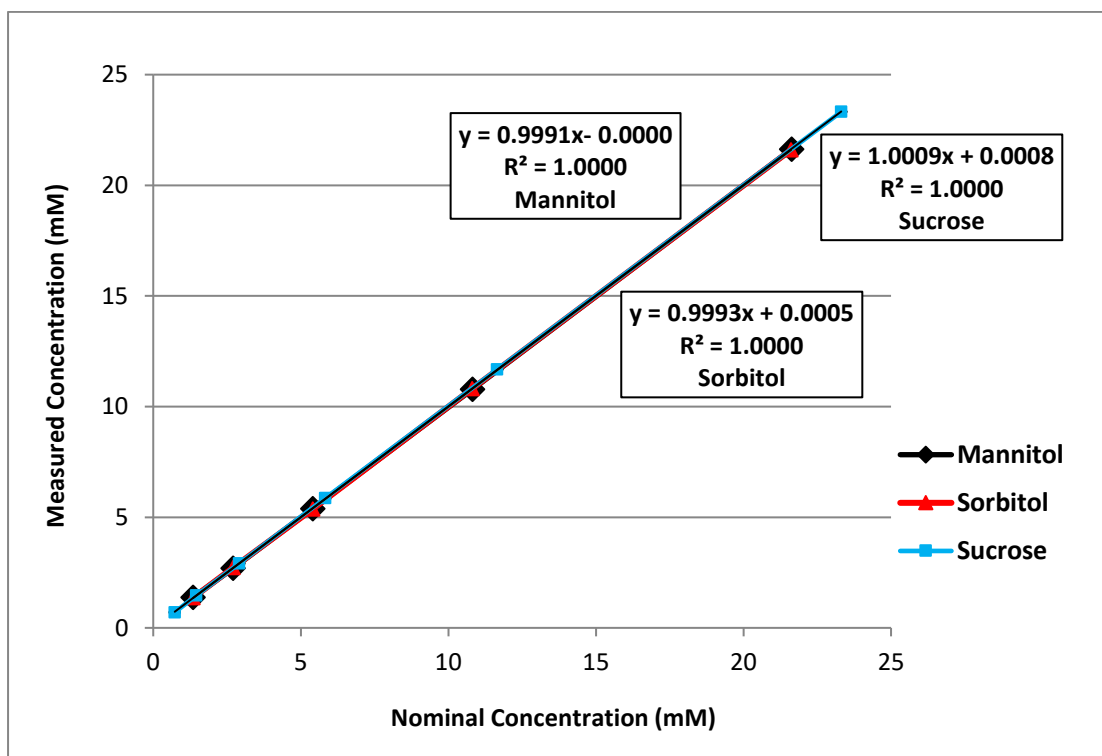


**Figure 6b:** Correction factors between nominal concentration (mM) and measured concentration (mM) for mannitol, sucrose and sorbitol.



### Accuracy and Precision

The accuracy and precision of the  $^1\text{H}$  qNMR method was assessed at three different concentrations. Table 2 shows that relative error (%) for mannitol, sucrose and sorbitol were all less than 3.697%. SD and RSD% values determined for the three saccharides were all below 0.389 and below 3.126, respectively. These results demonstrated that the  $^1\text{H}$  qNMR method produced accurate (bias % <3.697) and precise data with high repeatability (RSD % <3.126) with linear relationship over the concentration range used.

**Table 2:** Results of relative error (%), intra-day precision (three different concentrations / three replicates each on the same day) and inter-day precision (9 NMR data acquisitions per concentration over 3 days) validation study for the determination of mannitol, sucrose and sorbitol. Data presented as mean measured concentration (mM) with standard deviation (SD), relative standard deviation (RSD%) and relative error% (bias%).

Saccharide	Nominal concentration (mM)	Mean measured concentration (mM)	SD	RSD (%)	Relative error (%) (bias %)
Intra-day precision					
Mannitol	21.529	21.599	0.061	0.281	0.328
	5.382	5.449	0.025	0.464	1.234
	1.346	1.383	0.007	0.497	2.760
Sucrose	23.302	23.611	0.198	0.841	1.327
	5.825	5.880	0.020	0.338	0.940
	0.728	0.728	0.013	1.748	-0.054
Sorbitol	21.540	21.341	0.094	0.440	-0.924
	5.385	5.384	0.040	0.743	-0.014
	1.346	1.364	0.015	1.080	1.350
Inter-day precision					
Mannitol	21.529	21.568	0.112	0.517	0.184
	5.382	5.450	0.065	1.197	1.255
	1.346	1.395	0.011	0.789	3.697
Sucrose	23.302	23.962	0.389	1.625	2.831
	5.825	6.016	0.121	2.018	3.264
	0.728	0.741	0.023	3.126	1.755
Sorbitol	21.540	21.072	0.248	1.176	-2.173
	5.385	5.383	0.044	0.815	-0.045
	1.346	1.378	0.013	0.932	2.376

### Limit of detection (LOD) and limit of quantitation (LOQ)

LOD and LOQ values for all three saccharides are presented in Table 3. The results of LOD and LOQ show that the  $^1\text{H}$  qNMR method demonstrated significant sensitivity with low values of LOD (0.058 mM for mannitol, 0.045 mM for sucrose, and 0.056 mM for sorbitol) and LOQ (0.175 mM for mannitol, 0.135 mM for sucrose, and 0.168 mM for sorbitol). This indicates that concentrations determined from the linear concentration range of the calibration curves were both within LOD and LOQ.

**Table 3:** Linear correlation coefficient ( $R^2$ ), regression equation, limit of detection (LOD) and limit of quantitation (LOQ)

Saccharide	Regression equation for calibration curve	$R^2$	LOD (mM)	LOQ (mM)	Regression equation for correction factor
Mannitol	$y = 0.0417x - 0.0009$	1.0000	0.058	0.175	$y = 0.9991x - 0.0000$
Sucrose	$y = 0.0394x + 0.0014$	1.0000	0.045	0.135	$y = 1.0009x + 0.0008$
Sorbitol	$y = 0.0421x - 0.0007$	1.0000	0.056	0.168	$y = 0.9993x + 0.0005$

### 3.3. Pulmonary deposition study and saccharide quantification

The impaction study was carried out using a NGI equipped with an AIT 28028 in order to determine the amount of all three selected raw saccharides (mannitol, sucrose, and sorbitol) and SFD and SD dry powders composed of mannitol and sucrose deposited on AIT and all NGI stages using the calibration curve constructed by  $^1\text{H}$  qNMR analysis (Figure 6a).

In this study, with the exception of SD mannitol, six saccharide carrier formulations (raw mannitol, SFD mannitol, raw sucrose, SFD sucrose, SD sucrose and raw sorbitol) with over 50% of the cumulative mass deposited on AIT and stage 1 of the NGI with 11.719  $\mu\text{m}$  cut-off diameter, whereas below 50% of the total particles by mass deposited on between stage 2 with 6.395  $\mu\text{m}$  cut-off diameter and stage 7 with 0.541  $\mu\text{m}$  cut-off diameter and MOC in the NGI (Figure 7). Therefore, MMAD was reported as NA (no available values for one side of the 50% MMAD) and consequently GSD was reported as NA (Table 4). On the other hand, SD mannitol generated MMAD of  $5.778 \pm 0.348 \mu\text{m}$  (Table 4) as SD mannitol dry powders also deposited on the NGI stages between 2 and MOC. This could be due to the small particles prepared by SD (2-10  $\mu\text{m}$  by SEM and 5.54  $\mu\text{m}$  VMD by laser diffraction). However, there was no significant difference in the deposition pattern in AIT and stage 1 (representing the oropharynx region) between all saccharide formulations (one-way ANOVA,  $p > 0.05$ ). In contrast to the deposition pattern in AIT and stage 1, particles deposition with below 6.395  $\mu\text{m}$  cut-off diameter (stage 2) was dependent on the method of dry powder preparation that represented a significant difference in deposition patterns in the lower NGI stages (one-way ANOVA,  $p < 0.05$ ). This could be due to the various particle size and morphologies observed (Figure 1 and 2 and Table 1) that affected the powder deposition pattern.

FPF (aerodynamic diameter  $\leq 5.0 \mu\text{m}$ ) based on the saccharide deposition dose was determined for SD mannitol ( $23.714 \pm 3.659\%$ ), SFD mannitol ( $11.386 \pm 0.760\%$ ) and raw sucrose ( $1.537 \pm 0.443\%$ ) (Table 4) with high cumulative fraction between stage 3 and 5 (Table 5) where generally represents the desired deep lung regions for systemic pulmonary delivery. This presents that SD mannitol, SFD mannitol and raw sucrose dry powders would likely reach the lungs *in vivo* due to the presence of fine particles (aerodynamic diameter  $\leq 5.0 \mu\text{m}$ ) and could lead to the safety concern or alternatively could facilitate the efficiency of drug aerosolisation as mentioned in introduction. SD mannitol showed higher FPF than SFD mannitol indicating that higher amounts of mannitol dry powders prepared by SD deposited on the lower NGI stages compared with mannitol dry powders prepared by SFD. This represents that more SD dry powders would be expected to reach the lungs. However, raw mannitol, SFD sucrose, SD sucrose and raw sorbitol generated no FPF values reported by the NGI software (Table 4) due to a coarse-narrow distribution that over 50% of the cumulative mass deposited on AIT and stage 1 ( $> 11.719 \mu\text{m}$ ) and cumulative fraction of saccharide deposited on the lower NGI stages (2-7) was less than 1% per stage or only one stage had a cumulative fraction over 1% (i.e., 1.19% for raw mannitol) (Figure 7 and Table 5). This represents that these four different saccharide dry powders exhibited the oropharyngeal deposition in the oropharynx region, which is advantageous as DPI carriers. The delivered dose was in the order of raw sorbitol (69.93%) > SFD mannitol (68.99%) > SFD sucrose (66.62%) > SD sucrose (57.70%) > raw mannitol (57.25%) > SD mannitol (49.03%) > raw sucrose (43.35%) (Table 4). In this study, SFD mannitol and SFD sucrose with high moisture content (5.5% and 7.5%, respectively) exhibited better delivered dose than SD mannitol and SD sucrose with lower

moisture content (2% and 3%, respectively) (Table 4 and Figure 3). This indicated that the saccharide flowability was not dependent on the moisture content. Dry powders prepared as DPI carriers by SFD exhibited better flowability than dry powders prepared by SD. This could be due to the porous and fluffy particles produced by SFD that would have reduced inter-particulate forces resulting in better fluidisation (D'Addio *et al.*, 2013; Rahimpour, Kouhsoltani and Hamishehkar, 2014; Weers and Miller, 2015). Raw sorbitol exhibited the highest delivered dose with 69.93% among raw saccharides (57.25% for raw mannitol and 43.35% for raw sucrose). Raw mannitol exhibited higher delivered dose compared to SD mannitol. This could be due to the rough surface observed by SEM (Figure 1A and 2D) that would have been associated with reduced inter-particulate cohesive forces. The *in vitro* pulmonary deposition study demonstrated that SD and SFD produced saccharide dry powders with different deposition. The SFD method for saccharide dry powders preparation as DPI carriers seems to be more advantageous than SD as SFD exhibited higher delivered dose than SD.

**Table 4:** Delivered dose (%), fine particle fraction (FPF  $\leq 5.0 \mu\text{m}$ ), mass median aerodynamic diameter (MMAD) and geometric standard deviation (GSD) of raw mannitol, spray dried (SD) mannitol, spray freeze dried (SFD) mannitol, raw sucrose, spray dried (SD) sucrose, spray freeze-dried (SFD) sucrose and raw sorbitol dry powders assessed by Next Generation Impactor analysis at flow rate of  $30 \pm 0.5 \text{ L min}^{-1}$ . (Data presented as mean  $\pm$  standard deviation,  $n=3$ )

Saccharide carrier formulation	Dose		Size distribution	
	Delivered dose (%)	FPF (%)	MMAD ( $\mu\text{m}$ )	GSD
Raw mannitol	57.25	0	NA	NA
SD mannitol	49.03	$23.714 \pm 3.659$	$5.778 \pm 0.348$	$2.106 \pm 0.081$
SFD mannitol	68.99	$11.386 \pm 0.760$	NA	NA
Raw sucrose	43.35	$1.537 \pm 0.443$	NA	NA
SD sucrose	57.70	0	NA	NA
SFD sucrose	66.62	0	NA	NA
Raw sorbitol	69.93	0	NA	NA

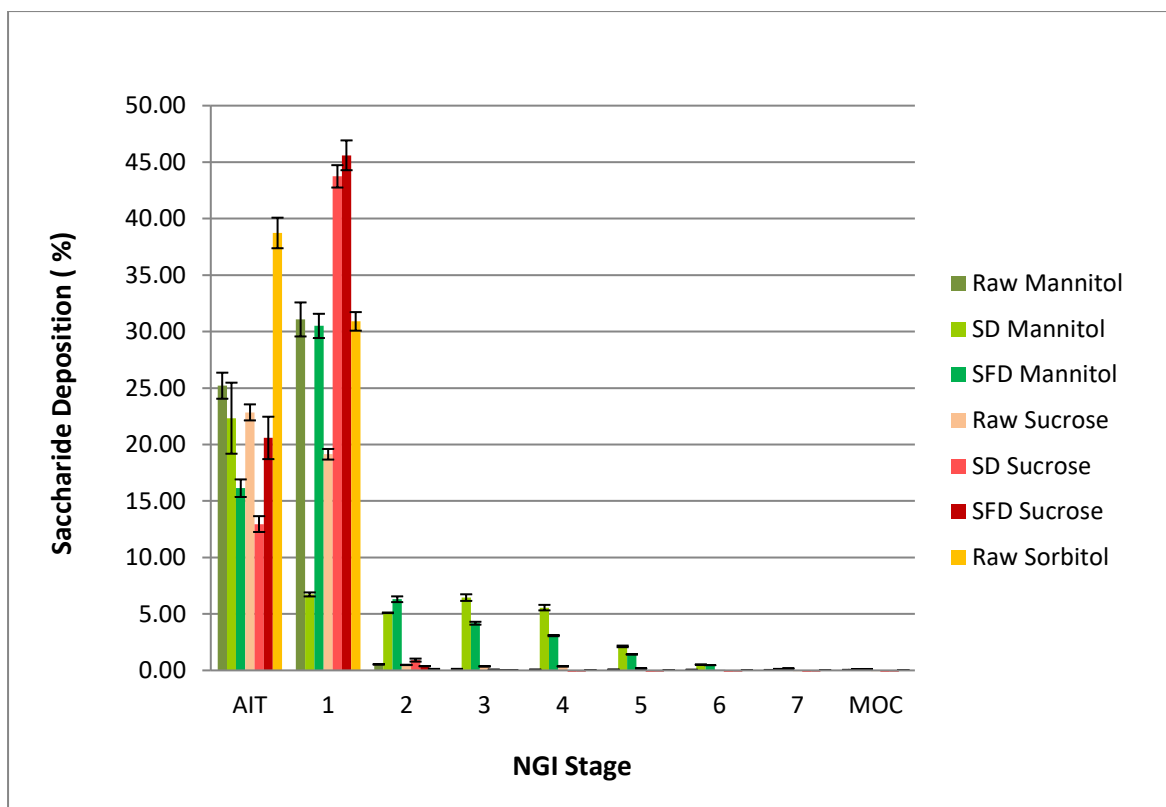


**Figure 7:** Particle size distribution by Next Generation Impactor (NGI) analysis at flow rate of  $30 \pm 0.5 \text{ L min}^{-1}$  for raw mannitol, spray dried (SD) mannitol, spray freeze dried (SFD) mannitol, raw sucrose, spray dried (SD) sucrose, spray freeze dried (SFD) sucrose and raw sorbitol. Saccharide deposition is expressed as delivered dose (%) per NGI stage. (Data presented as mean  $\pm$  standard deviation,  $n=3$ ) AIT: Alberta idealised throat, MOC: Micro orifice collector.

**Table 5:** Cumulative fraction (%) of raw mannitol, spray dried (SD) mannitol, spray freeze dried (SFD) mannitol, raw sucrose, spray dried (SD) sucrose, spray freeze dried (SFD) sucrose and raw sorbitol deposited on Next Generation Impactor (NGI) stages (1-7). Cumulative fraction per NGI stage was calculated by the Copley Inhaler Testing Data Analysis software based on summation of the cumulative mass collected on NGI stages (1-7 and MOC, Alberta idealised throat is not included). (Data presented as mean,  $n=3$ )

NGI Stage (Cut-off diameter)	Cumulative fraction (%)						
	Raw Mannitol	SFD Mannitol	SD Mannitol	Raw Sucrose	SFD Sucrose	SD Sucrose	Raw Sorbitol
1 (11.719 $\mu\text{m}$ )	2.87	34.03	74.78	6.71	1.10	2.51	0.90
2 (6.395 $\mu\text{m}$ )	1.19	20.40	55.65	4.34	0.16	0.34	0.51
3 (3.988 $\mu\text{m}$ )	0.78	11.37	31.53	2.58	0.00	0.00	0.42
4 (2.299 $\mu\text{m}$ )	0.60	4.71	10.74	0.82	0.00	0.00	0.34
5 (1.357 $\mu\text{m}$ )	0.41	1.64	2.78	0.00	0.00	0.00	0.26
6	0.25	0.63	0.88	0.00	0.00	0.00	0.17

(0.834 $\mu\text{m}$ )							
7 (0.541 $\mu\text{m}$ )	0.13	0.27	0.39	0.00	0.00	0.00	0.09

## 4. Conclusion

The  $^1\text{H}$  qNMR method was developed to quantify saccharides employed in DPI formulations and produced accurate and precise data with high repeatability within the calibration curve concentration range. The present study demonstrated the quantification of the three saccharide DPI carriers (raw, SFD and SD) using the developed  $^1\text{H}$  qNMR method and the lung deposition patterns *in vitro* for saccharide DPI carriers were assessed based on the amount of deposited saccharide quantified at each stage of the NGI. There was a significant difference in deposition patterns in the lower NGI stages (stage 2, <6.395  $\mu\text{m}$  cut-off diameter) between all saccharide formulations. These differences could be due to the various particle size and morphologies observed with the use of different methods of dry powder preparation (raw, SFD and SD) that affected the powder deposition pattern. In contrast to the deposition patterns in the lower NGI stages, there was no significant difference in the deposition pattern in AIT and stage 1 (representing the oropharynx region) between all saccharide formulations. In this study, raw mannitol, SD sucrose, SFD sucrose and raw sorbitol exhibited the oropharyngeal deposition in the oropharynx region, which is advantageous as DPI carriers whereas SD mannitol, SFD mannitol and raw sucrose dry powders would likely reach the lungs *in vivo* due to the presence of fine particles (aerodynamic diameter  $\leq 5.0 \mu\text{m}$ ). SFD mannitol showed the particle deposition both in the oropharynx region and deep lung regions for systemic pulmonary delivery due to high span value. SD D-mannitol showed higher FPF than SFD D-mannitol. This was measured by the NGI depositions studies where  $^1\text{H}$  qNMR showed that higher amounts of SD mannitol dry powders deposited on the lower NGI stages compared with SFD mannitol dry powders. So it can be estimated that more SD saccharide dry powders would be expected to reach the lungs. It was found that the saccharide powder flowability was not dependent on the moisture content as SFD mannitol and SFD sucrose with high moisture content exhibited better delivered dose than SD mannitol and SD sucrose with lower moisture content. This could be due to the porous (and fluffy) particles produced by SFD. The developed  $^1\text{H}$  qNMR methodology can be used as an analytical method to assess pulmonary deposition in impaction experiments of saccharides employed as carriers in DPI formulations and ensure avoidance of saccharides deep deposition in lung.

**Funding Statement:** This research did not receive any specific grant from funding agencies in the public, commercial, or not-for-profit sectors.

**Author Disclosures:** The authors have no competing interests to declare.

## References

- Ali, N. and Gary, P.M. 2015, Pulmonary Drug Delivery: Advances and Challenges, United Kingdom: John Wiley & Sons Inc.
- Al-Tabakha, M., 2015. Future prospect of insulin inhalation for diabetic patients: The case of Afrezza versus Exubera. *Journal of Controlled Release*, 215, pp. 25-38.
- Balducci, A.G., Cagnani, S., Sonvico, F., Rossi, A., Barata, P., Colombo, G., Colombo, P. & Buttini, F. 2014, "Pure insulin highly respirable powders for inhalation", *European Journal of Pharmaceutical Sciences*, vol. 51, pp. 110-117.
- Banga, A.K. 2015, Therapeutic peptides and proteins: formulation, processing, and delivery systems, 2nd edn. Boca Raton, Florida; London, England; New York: CRC Press.

- Berkenfeld, K., Lamprecht, A. and McConville, J. 2015, "Devices for Dry Powder Drug Delivery to the Lung", *AAPS PharmSciTech*, vol. 16, no. 3, pp. 479-490.
- Bharti, S.K. and Roy, R., 2012. Quantitative <sup>1</sup>H NMR spectroscopy. *Trends in Analytical Chemistry*, 35, pp. 5-26.
- Chiara Pietrogrande, M., Barbaro, E., Bove, M.C., Clauser, G., Colombi, C., Corbella, L., Cuccia, E., Dalla Torre, S., Decesari, S., Fermo, P., Gambaro, A., Gianelle, V., Ielpo, P., Larcher, R., Lazzeri, P., Massabò, D., Melchionna, G., Nardin, T., Paglione, M., Perrino, C., Prati, P., Visentin, M., Zanca, N. and Zangrando, R., 2017. Results of an interlaboratory comparison of analytical methods for quantification of anhydrosugars and biosugars in atmospheric aerosol. *Chemosphere*, 184, pp. 269-277.
- Coombes, S.R., Hughes, L.P., Phillips, A.R. & Wren, S.A.C. 2014, "Proton NMR: a new tool for understanding dissolution", *Analytical Chemistry*, vol. 86, no. 5, pp. 2474.
- D'addio, S., Chan, J., Kwok, P., Benson, B., Prud'homme, R. and Chan, H., 2013. Aerosol Delivery of Nanoparticles in Uniform Mannitol Carriers Formulated by Ultrasonic Spray Freeze Drying. *Pharmaceutical research*, 30(11), pp. 2891-2901.
- Depreter, F., Pilcer, G. & Amighi, K. 2013, "Inhaled proteins: Challenges and perspectives", *International journal of pharmaceutics*, vol. 447, no. 1-2, pp. 251-280.
- Duru, C., Swann, C., Dunleavy, U., Mulloy, B. & Matejtschuk, P. 2015, "The importance of formulation in the successful lyophilization of influenza reference materials", *Biologicals*, vol. 43, no. 2, pp. 110-116.
- Farizhandi, A.A.K., Paćłowski, A., Szłęk, J., Mendyk, A., Shao, Y. & Lau, R. 2019, "Evaluation of carrier size and surface morphology in carrier-based dry powder inhalation by surrogate modeling", *Chemical Engineering Science*, vol. 193, pp. 144-155
- Giraudeau, P., Silvestre, V. and Akoka, S. 2015, Optimizing water suppression for quantitative NMR-based metabolomics: a tutorial review.
- Günther, H., 2013. *NMR spectroscopy: basic principles, concepts, and applications in chemistry*. Siegen: Wiley-VCH.
- Hamishehkar, H., Emami, J., Najafabadi, A.R., Gilani, K., Minaian, M., Mahdavi, H. and Nokhodchi, A., 2010. Effect of carrier morphology and surface characteristics on the development of respirable PLGA microcapsules for sustained-release pulmonary delivery of insulin. *International journal of pharmaceutics*, 389(1), pp. 74-85.
- Holzgrabe, U., 2010. Quantitative NMR spectroscopy in pharmaceutical applications. *Progress in Nuclear Magnetic Resonance Spectroscopy*, 57(2), pp. 229-240.
- Hore, P.J., 1983. A new method for water suppression in the proton NMR spectra of aqueous solutions. *Journal of Magnetic Resonance* (1969), 54(3), pp.539-542.
- Hou, Z., Liang, X., Du, L., Su, F. and Su, W., 2014. Quantitative determination and validation of avermectin B 1a in commercial products using quantitative nuclear magnetic resonance spectroscopy. *Magnetic Resonance in Chemistry*, 52(9), pp. 480-485.
- Kaialy, W. and Nokhodchi, A. 2012, "Antisolvent crystallisation is a potential technique to prepare engineered lactose with promising aerosolisation properties: Effect of saturation degree", *International journal of pharmaceutics*, vol. 437, no. 1-2, pp. 57-69.
- Karner, S., Littringer, E.M. and Urbanetz, N.A., 2014. Triboelectrics: The influence of particle surface roughness and shape on charge acquisition during aerosolization and the DPI performance. *Powder Technology*, 262, pp. 22-29.
- Kramek-Romanowska, K., Odziomek, M., Sosnowski, T.R. and Gradoń, L. 2011, "Effects of process variables on the properties of spray-dried mannitol and mannitol/disodium cromoglycate powders suitable for drug delivery by inhalation", *Industrial and Engineering Chemistry Research*, vol. 50, no. 24, pp. 13922-13931.
- Maltesen, M., Weert, M. and Grohgan, H. 2012, "Design of Experiments-Based Monitoring of Critical Quality Attributes for the Spray-Drying Process of Insulin by NIR Spectroscopy", *AAPS PharmSciTech*, vol. 13, no. 3, pp. 747-755.
- Mönckedieck, M., Kamplade, J., Fakner, P., Urbanetz, N.A., Walzel, P., Steckel, H. & Scherließ, R. 2017, "Dry powder inhaler performance of spray dried mannitol with tailored surface morphologies as carrier and salbutamol sulphate", *International journal of pharmaceutics*, vol. 524, no. 1-2, pp. 351-363.
- Nezzal, A., Aerts, L., Verspaille, M., Henderickx, G. & Redl, A. 2009, "Polymorphism of sorbitol", *Journal of Crystal Growth*, vol. 311, no. 15, pp. 3863-3870.

- Niwa, T., Mizutani, D. and Danjo, K. 2012. Spray Freeze-Dried Porous Microparticles of a Poorly Water-Soluble Drug for Respiratory Delivery. *Chemical and Pharmaceutical Bulletin*, 60(7), pp.870-876.
- Pauli, G., Godecke, T., Jaki, B. and Lankin, D.C., 2012. Quantitative <sup>1</sup>H NMR. Development and Potential of an Analytical Method: An Update.
- Peng, T., Lin, S., Niu, B., Wang, X., Huang, Y., Zhang, X., Li, G., Pan, X. and Wu, C. 2016, "Influence of physical properties of carrier on the performance of dry powder inhalers", *Acta Pharmaceutica Sinica B*, vol. 6, no. 4, pp. 308-318.
- Pilcer, G. & Amighi, K. 2010, "Formulation strategy and use of excipients in pulmonary drug delivery", *International journal of pharmaceutics*, vol. 392, no. 1, pp. 1-19.
- Rahimpour, Y., Kouhsoltani, M. and Hamishehkar, H., 2014. Alternative carriers in dry powder inhaler formulations. *Drug discovery today*, 19(5), pp. 618-626.
- Razavi Rohani, S.S., Abnous, K. and Tafaghodi, M., 2014. Preparation and characterization of spray-dried powders intended for pulmonary delivery of Insulin with regard to the selection of excipients. *International journal of pharmaceutics*, 465(1-2), pp. 464-478.
- Richards, S., and Hollerton, J. C., 2011. *Essential practical NMR for organic chemistry*. Chichester, West Sussex, U.K.: John Wiley.
- Roberts, G., and Lian, LY., 2011. *Protein NMR Spectroscopy Practical Techniques and Applications*. Chichester; Hoboken: Chichester: Wiley.
- Santos Cavaiola, T. and Edelman, S. 2014, "Inhaled Insulin: A Breath of Fresh Air? A Review of Inhaled Insulin", *Clinical therapeutics*, vol. 36, no. 8, pp. 1275-1289.
- Schievano, E., Tonoli, M. & Rastrelli, F. 2017, "NMR Quantification of Carbohydrates in Complex Mixtures. A Challenge on Honey", *Analytical Chemistry*, vol. 89, no. 24, pp. 13405.
- Schmid, T., Baumann, B., Himmelsbach, M., Klampfl, C. and Buchberger, W. 2016, "Analysis of saccharides in beverages by HPLC with direct UV detection", *Analytical and Bioanalytical Chemistry*, vol. 408, no. 7, pp. 1871-1878.
- Simmler, C., Napolitano, J.G., Mcalpine, J.B., Chen, S. and Pauli, G.F., 2014. Universal quantitative NMR analysis of complex natural samples. *Current opinion in biotechnology*, 25, pp. 51-59.
- Sterling, C., Crouch, R., Russell, D.J. and Calderón, A.I., 2013. <sup>1</sup>H-NMR Quantification of Major Saccharides in Açai Raw Materials: a Comparison of the Internal Standard Methodology with the Absolute Intensity qNMR Method. *Phytochemical Analysis*, 24(6), pp. 631-637.
- Ung, K.T., Rao, N., Weers, J.G., Clark, A.R. and Chan, H. 2014, "In Vitro Assessment of Dose Delivery Performance of Dry Powders for Inhalation", *Aerosol Science and Technology*, 48(10), pp.1099-1110.
- Wallmeier, J., Samol, C., Ellmann, L., Zacharias, H.U., Vogl, F.C., Garcia, M., Dettmer, K., Oefner, P.J. and Gronwald, W., 2017. Quantification of Metabolites by NMR Spectroscopy in the Presence of Protein. *Journal of Proteome Research*, 16(4), pp. 1784-1796.
- Walters, R.H., Bhatnagar, B., Tchessalov, S., Izutsu, K., Tsumoto, K. and Ohtake, S., 2014. Next Generation Drying Technologies for Pharmaceutical Applications. *Journal of pharmaceutical sciences*, 103(9), pp. 2673-2695.
- Weers, J.G. and Miller, D.P., 2015. Formulation Design of Dry Powders for Inhalation. *Journal of pharmaceutical sciences*, 104(10), pp. 3259-3288.
- Yamazaki, T. and Takatsu, A. 2014, "Quantitative NMR spectroscopy for accurate purity determination of amino acids, and uncertainty evaluation for different signals", *Accreditation and Quality Assurance*, vol. 19, no. 4, pp. 275-282.
- Yang, M.Y., Chan, J.G.Y. & Chan, H. 2014, "Pulmonary drug delivery by powder aerosols", *Journal of Controlled Release*, vol. 193, pp. 228-240.